

Radiative capture of orbital electrons in the decay of ${}^7\text{Be}$

H. Sanjeeviah and B. Sanjeevaiah

Department of Physics, University of Mysore, Manasagangotri, Mysore 570 006, India

(Received 10 August 1977)

The higher energy portion of the inner bremsstrahlung spectrum accompanying the allowed orbital electron capture transition in ${}^7\text{Be}$ to the ground state of ${}^7\text{Li}$ was measured with a single channel NaI(Tl) scintillation spectrometer. Correction for the pileup spectrum due to the 478 keV nuclear γ rays arising from the deexcitation of the first excited state in ${}^7\text{Li}$ was performed by numerical integration. The measured pulse-height distribution of the inner bremsstrahlung photons was corrected for detector response following the procedures of Liden and Starfelt and Palmer and Laslett. For energies higher than 560 keV the number of $1S + 2S$ bremsstrahlung photons emitted per ground state EC decay of ${}^7\text{Be}$ was determined to be $(6.31 \pm 0.38) \times 10^{-5}$. Corresponding theoretical values are 6.46×10^{-5} , deduced from Martin-Glauber theory, and 6.45×10^{-5} , deduced from the improved calculations of Intemann. The present result is in good agreement with the theoretical predictions. The decay energy of ${}^7\text{Be}$ was determined to be 857 ± 14 in agreement with the accepted atomic mass difference.

[RADIOACTIVITY ${}^7\text{Be}$; measured inner bremsstrahlung, γ ; deduced I_{IB} , Q .
NaI(Tl) detector, numerical integration method.]

I. INTRODUCTION

When a nucleus decays by capturing an orbital electron (EC) there is a small probability that this process is accompanied by the simultaneous emission of electromagnetic radiation, usually referred to as inner bremsstrahlung (IB). Moller¹ and Morrison and Schiff² independently developed the theory of IB spectra in allowed transitions, completely neglecting the influence of the nuclear Coulomb field. This theory is restricted to $1S$ -state capture and it predicts a differential spectrum of the form $x(x_0 - x)^2$, where x is the energy of the emitted photon and x_0 is the end point.

Inner bremsstrahlung from orbital electron capture was first observed by Bradt *et al.*³ in ${}^{55}\text{Fe}$. A number of workers have reported the measurement of IB at higher energies. All these data were consistent with the Morrison-Schiff theory.⁴ When measurements were extended to include IB photon distribution at lower energies, however, an unexpected steep rise of IB intensity was noticed.^{5,6} Martin and Glauber^{7,8} carried out extensive calculations for allowed capture from both K and L shells taking into account the nuclear Coulomb field and relativistic and screening effects. The new theory successfully explained the observed excess of low energy photons in IB intensity as due to capture of electrons from the L shell. It provides approximate expressions for the calculation of the partial spectra corresponding to capture of electrons from the various orbital states. The total intensities of the spectra are related to the ordinary nonradiative $1S$ electron capture. The rel-

ativistic corrections appear as factors multiplying the nonrelativistic expressions for the S -state spectra. These factors do not affect noticeably the shapes of the spectra. The intensities of the spectra, however, depend crucially on their magnitudes.

A relatively simple procedure for calculating exact numerical results for the relativistic correction factors for arbitrary k and z has been developed by Intemann.⁹ Zon and Rapaport¹⁰ have generalized this theory to electron capture transitions of all degrees of forbiddenness.

The agreement between theory and experiment is not wholly satisfactory. The shapes of total spectra and partial $1S$ spectra have been measured for a number of allowed capture transitions between various nuclei and found to be in good agreement with theory.⁵ However, the intensities of these spectra, obtained mainly from IB- γ coincidences, show wide divergences from the theoretical predictions.⁶ Only Kadar, Berenyi, and Myslek¹¹ report agreement with theory.

Orbital electron capture decay of ${}^7\text{Be}$ is an excellent example for allowed low- Z transitions ($\Delta J=0$; $\Delta\pi=\text{no}$; $\log_{10}ft=3.36$) for which the calculations of Martin and Glauber are expected to be most accurate. The end point of the IB spectrum accompanying the ground state to ground state branch decay (89.7%) in this isotope falls well beyond the energy (478 keV) of the nuclear γ rays resulting from the decay in the other branch (10.3%). Therefore it becomes possible to measure accurately the IB spectrum in the higher energy region with a NaI(Tl) scintillation spectrometer. Further, correction for the pileup spec-

trum can be easily made by performing numerical integration.

IB accompanying ground state to ground state electron capture decay of ${}^7\text{Be}$ has been measured only once before with a Ge(Li) γ -ray spectrometer with a pileup rejector.¹² Agreement between theory and experiment was reported in contradiction to earlier measurements.^{13,14} Therefore it was thought worthwhile to reinvestigate the IB spectrum associated with the ground state to ground state electron capture decay of this isotope.

Accurate determination of the intensities of inner bremsstrahlung are also relevant for experiments aimed at determining the parity mixtures¹⁵ in nuclear states, testing basic features of the theory of weak interactions, and precise γ counting.¹⁶

II. EXPERIMENTS

The decay scheme of ${}^7\text{Be}$ and the experimental setup are shown in Fig. 1. The inner bremsstrahlung spectrum accompanying the ground state to ground state transition in ${}^7\text{Be}$ was measured in the energy region 560–820 keV with a NaI(Tl) scintillation spectrometer. The source was obtained in the form of carrier-free ${}^7\text{BeCl}_2$ solution from Radiochemical Centre, Amersham, U.K. A known quantity of the solution was evaporated, drop by drop, on a thin aluminated Mylar film (~ 2 mg cm^{-2}) mounted on a Perspex ring of inner diameter 2.4 cm. Sufficient care was taken to have uniform spread using a drop or two of dilute aqueous solution of insulin and the extent of the source was limited to a circular area of 0.6 cm diam. In all, three sources of low activity (~ 1.7 μCi) and two of higher activity (~ 50 μCi) were used in the present study.

Counts were accumulated in each channel, once with the source in position and again without it in position. Counting time was varied from 5000 to 50000 sec according to the energy region of the measured IB pulse-height distribution. The background level was greatly minimized by housing the NaI(Tl) crystal-photomultiplier assembly in a lead shield of wall thickness 8.4 cm. To reduce the pileup of uncorrelated pulses a lead filter of thickness 1.2 mm was placed in between the detector and the source.¹⁷ The linearity of the analyzer was checked by using the following γ -ray lines: 280 keV (${}^{203}\text{Hg}$), 412 keV (${}^{198}\text{Au}$), 662 keV (${}^{137}\text{Cs}$), 835 keV (${}^{54}\text{Mn}$), and 1114 keV (${}^{65}\text{Zn}$). It was found to be good within 1%. The stability of the counting system was ensured by using a stabilized power supply and maintaining the laboratory temperature constant at 23 ± 1 °C. It was checked before and after each individual run by means of an 835 keV

γ -ray line of ${}^{54}\text{Mn}$.

In order to estimate the contributions from the impurity isotopes (${}^{65}\text{Zn}$, ${}^{88}\text{Y}$, ${}^{48}\text{V}$, ${}^{54}\text{Mn}$, and ${}^{22}\text{Na}$ ¹²) to the measured IB spectra we obtained the entire spectra (0–2 MeV) of the stronger sources with a Ge(Li) spectrometer. Contributions from ${}^{48}\text{V}$ and ${}^{22}\text{Na}$ γ rays were scarcely seen ($\leq 10^{-6}$). Contributions from the other isotopes were found to be less than 10^{-3} of the transition rate to the first excited state of ${}^7\text{Li}$. γ -ray spectra of impurity isotopes ${}^{65}\text{Zn}$ and ${}^{54}\text{Mn}$ were recorded and after proper intensity normalization, subtracted from the ${}^7\text{Be}$ spectrum. With regard to the impurity peak due to ${}^{88}\text{Y}$ γ rays the spectrum of ${}^{54}\text{Mn}$ γ rays was itself shifted in energy scale, making proper adjustment for the change in the resolution¹⁸ and intensity,¹⁹ and subtracted from the ${}^7\text{Be}$ spectrum. This procedure was adopted because of the non-availability of the ${}^{88}\text{Y}$ source in our laboratory. Only the correction due to the ${}^{54}\text{Mn}$ γ rays was important. The total contribution to the measured IB from the impurity isotopes was less than 10%.

III. EVALUATION OF THE IB SPECTRA

The measured counting rate $n_{ab}(E_r)$ in each channel above the photopeak is the sum of counts from pileup $n_p(E_r)$, inner bremsstrahlung $n_{IB}(E_r)$, and background $n_B(E_r)$:

$$n_{ab}(E_r) = n_p(E_r) + n_{IB}(E_r) + n_B(E_r). \quad (3.1)$$

Contributions to the pileup come predominantly from the photopeak region. Therefore, restricting to first order summing, we may write¹⁷

$$n_p(E_r) = 2\tau \int_0^{E_r} N(E_r - x)N(x) dx, \quad (3.2)$$

where τ is the resolving time of the detecting system and $N(E_r - x)$ and $N(x)$ are the numbers of photons with energy $(E_r - x)$ and x , respectively. The integration in Eq. (3.2) is performed numerically to obtain $n_p(E_r)$ at each channel. The background counting rate and the calculated pileup counting rate were subtracted from the measured counting rate.

In order to obtain the true IB spectrum the background and pileup corrected spectrum should be further corrected for detector response. This is done either by constructing the response matrix of the detector and using it for spectral unfolding or by following the procedure due to Liden and Starfelt.²⁰ In the present study we have followed Liden and Starfelt procedure. This consists in correcting for dead-time counting loss, finite energy resolution, Compton electron distribution, iodine K x-ray escape, backscattering, γ detection efficiency and geometry in that order.

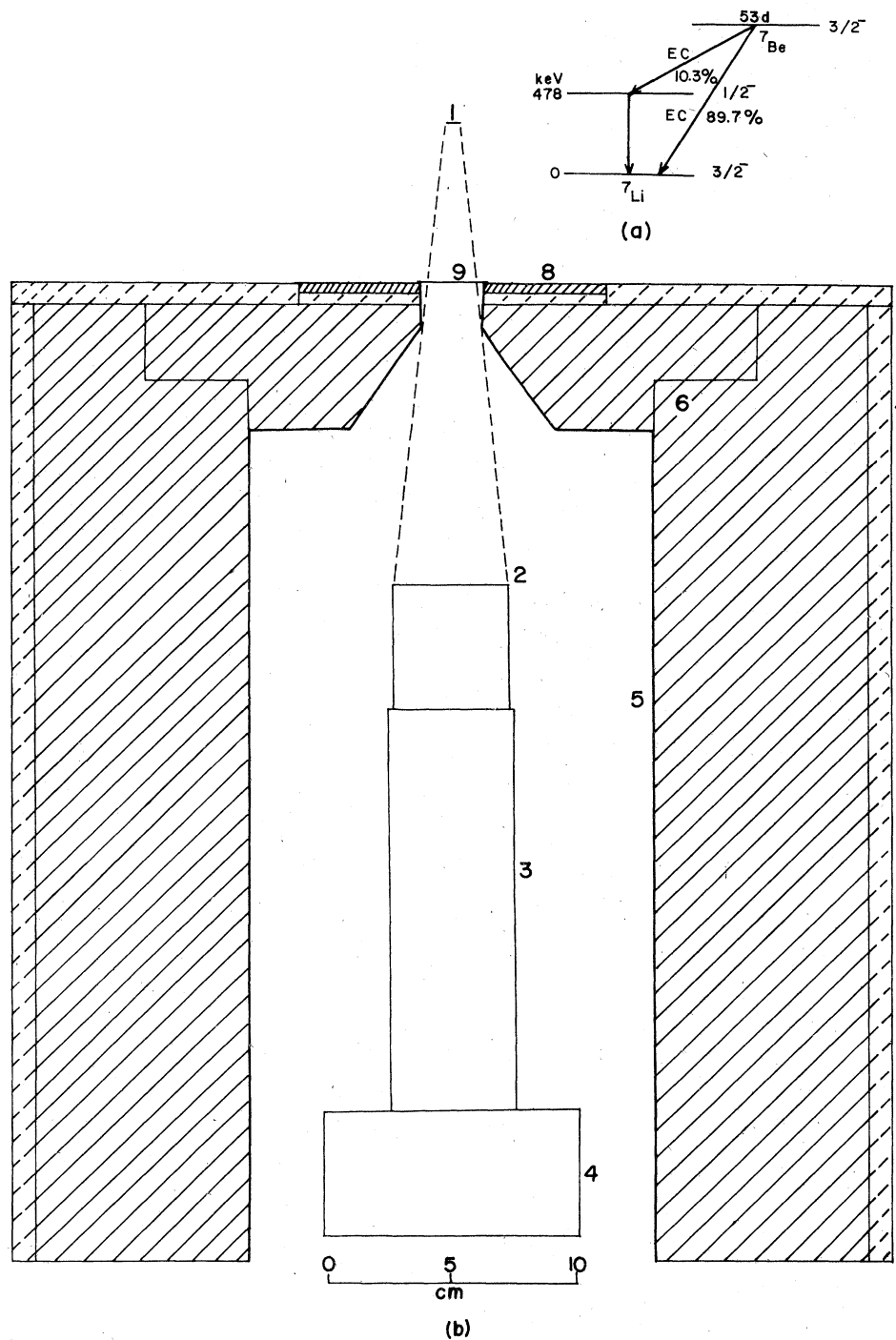


FIG. 1. (a) Decay scheme of ${}^7\text{Be}$. (b) Experimental setup: 1: source; 2: 5.1×4.4 cm NaI(Tl) crystal; 3: photo-multiplier; 4: cathode follower and preamplifier; 5: aluminum lining; 6: lead; 7: iron; 8: Perspex ring; and 9: 1:2 mm lead filter.

Correction for dead-time counting loss was found to be negligible because of the small resolving time ($4 \mu\text{sec}$) of the analyzer and small strengths of the sources used. The situation in connection

with the correction for finite energy resolution is very contradictory.²¹ In any case this correction must be more considerable at higher energies because of increasing experimental half widths of

the monoenergetic γ -ray lines with increasing energy. Most of the workers who have measured IB associated with β decay or electron capture have followed the procedure of Liden and Starfelt.^{19,21} But Dixon and Attken²² found this procedure to give incorrect estimates of the resolution correction. In recent years the other two procedures, one due to Owen and Primakoff²³ and other due to Palmer and Laslett²⁴ are being followed. Both these procedures lead to higher values for the correction, especially at the higher energy portion of the spectra desired.

In our measurement the correction for the finite energy resolution was made using the expression given by Palmer and Laslett:

$$n_{\text{corr}}(E_r) = n_{\text{IB}}(E_r) - k n'_{\text{IB}}(E_r) - \frac{1}{2} E_r n''_{\text{IB}}(E_r), \quad (3.3)$$

where $n'_{\text{IB}}(E_r)$ and $n''_{\text{IB}}(E_r)$ are the first and second derivatives of the background and pileup corrected spectrum $n_{\text{IB}}(E_r)dE_r$ at E_r and $k = W^2(E_r)/0.693.2E_r$ where $W(E_r)$ is the half width at half height of the photopeak produced by photons of energy E_r . The derivatives required were determined by means of the so called 7 multiplier method which is based on the fitting of the best third order curve. In the energy region of present interest the calculations of Owen and Primakoff also lead to the same result.

The correction for Compton electron distribution is considerable in the energy region below 600 keV.¹⁹ If the number of photons of energy E_r absorbed in the crystal is $n_a(E_r)$, then the number of Compton electrons having energies ranging from zero to E_r^* , the maximum energy of the recoil electron, is $n_a(E_r)[1 - K(E_r)]$, where $K(E_r)$ is the fraction of photons detected with full energy. The probability that such a Compton electron will have an energy between E and $E + \Delta E$ is a function $C(E, E_r)$. The total number of Compton electrons at energy E due to all incoming photons from zero to E_{max} is

$$n_c(E) = \int_0^{E_{\text{max}}} C(E, E_r) n_a(E_r) [1 - K(E_r)] dE_r \quad (3.4)$$

on the assumption that the Compton electron distribution for any γ -ray energy is approximately constant over the energy range from zero to E_r^* , the following approximation is made

$$C(E, E_r) = C(E_r) = \frac{1}{E_r^*} \quad \text{for } 0 < E < E_r^* \quad (3.5a)$$

and

$$C(E, E_r) = C(E_r) = 0 \quad \text{for } E > E_r^*. \quad (3.5b)$$

In order to obtain the Compton electron distribution the integration in Eq. (3.4) is performed numerically. Actually the observed pulse-height distribution is first extrapolated to the end point. By

starting at the highest energy, $n_a(E_r)$ is taken. Next the corresponding $[1 - K(E_r)]$ is calculated. Then by choosing a suitable value for ΔE_r , the ordinate $(\Delta n_c)_{E_r}$ of the Compton distribution from zero to E_r^* due to photons of energy between E_r and $E_r + \Delta E_r$ is calculated by the relation

$$(\Delta n_c)_{E_r} = \frac{1}{E_r^*} n_a(E_r) [1 - K(E_r)] \Delta E_r. \quad (3.6)$$

This process is repeated to cover the entire energy region. Finally, by adding up all the contributions, the Compton electron distribution is obtained. This is subtracted from the pileup, background, and finite energy resolution corrected IB pulse-height distribution.

The actual values of $K(E_r)$ can be determined from the experimental pulse-height distributions of a number of single γ -ray lines in the energy region of interest using the relation²⁵

$$K(E_r) = \frac{n_p(E_r)}{n_p(E_r) + n_c(E_r)}, \quad (3.7)$$

where $n_p(E)$ is the number of photons detected under the photopeak and $n_c(E_r)$ is the number of photons detected under the Compton continuum. In the present study $K(E_r)$ was determined by recording under the same geometrical arrangement complete spectra of monoenergetic γ -ray lines: 145 keV (¹⁴¹Ce), 280 keV (²⁰³Hg), 320 keV (⁵¹Cr), 412 keV (¹⁹⁸Au), 662 keV (¹³⁷Cs), 835 keV (⁵⁴Mn), and 1114 keV (⁶⁵Zn). The values of $K(E_r)$ thus obtained are shown in Fig. 2. The Compton electron distribution relevant to the measured pulse-height distribution was calculated using these values.

Correction for iodine K x-ray escape is important only in the energy region below 150 keV. Since our measurements were restricted to the region above 560 keV this correction was neglected.

The photons backscattered from the photomulti-

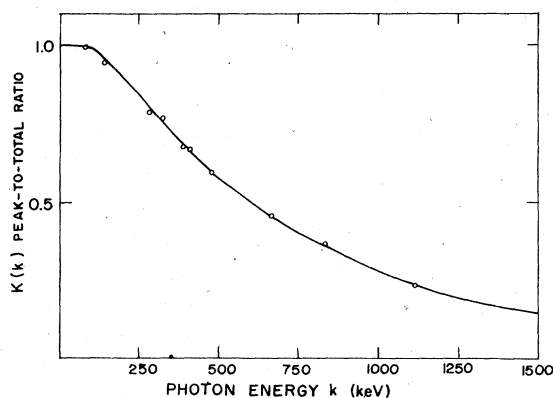


FIG. 2. Peak-to-total ratio vs γ -ray energy for the 5.08×4.45 cm NaI(Tl) detector.

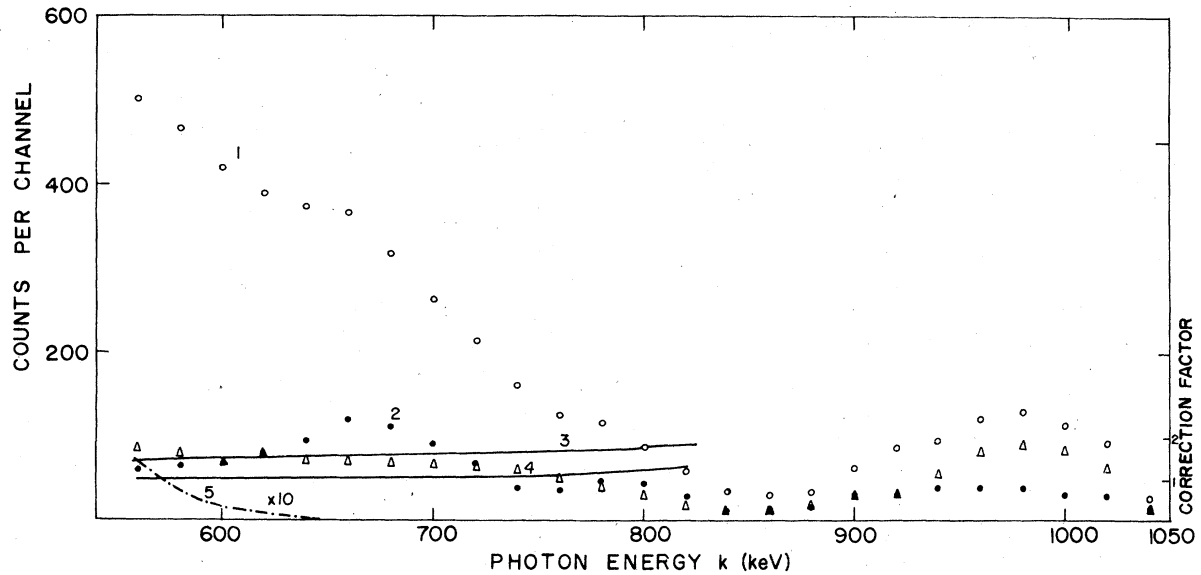


FIG. 3. 1: Experimental pulse-height distribution; 2: background; 3: correction factor for detection efficiency; 4: correction factor for energy resolution; 5: Compton electron distribution.

plier window, source backing, the crystal container, and the lead shield make undesirable contributions to the spectrum in the range 100–300 keV. Since the energy region of present interest is above 560 keV this correction was also neglected.

The most important correction relevant to the present measurement is the one due to γ detection efficiency. γ detection efficiency $\epsilon_p(E_\gamma)$ at any energy E_γ is given by the product of the peak-to-total ratio $K(E_\gamma)$ and the intrinsic efficiency $\epsilon_t(E_\gamma)$, i.e.,

$$\epsilon_p(E_\gamma) = K(E_\gamma)\epsilon_t(E_\gamma). \quad (3.8)$$

The values of the intrinsic efficiencies for our crystal were obtained from the theoretically computed data of Wolicki, Jastrow, and Brooks.²⁶ The pulse distribution corrected for detection efficiency is given by

$$n_{IB}^{exp}(E_\gamma) = n_p(E_\gamma)/\epsilon_p(E_\gamma), \quad (3.9)$$

where $n_p(E_\gamma)$ is the pulse distribution of the IB photons obtained after all the corrections, discussed before, are made.

The calculations of the source strength and the absolute intensity of the IB spectrum involve the same geometry factor. It cancels out when the number of IB photons per electron capture decay is calculated. Figure 3 shows the experimental pulse-height distribution, the background, pileup spectrum, Compton electron distribution, and the other correction factors.

IV. THEORY

${}^7\text{Be}$ decays through only 1S and 2S electron capture. Therefore the total theoretical IB spectrum is restricted to 1S+2S IB. According to the theory of Martin and Glauber, with low- Z approximations, the IB spectrum $W_{IB}^{th}(k)dk$ per electron capture decay in ${}^7\text{Be}$ can be calculated as

$$W_{IB}^{th}(k)dk = \frac{\alpha}{\pi} k dk [P_K(1 - k/k_{max}^{1S})^2 R_{1S}(z, k) + P_{L_1}(1 - k/k_{max}^{2S})^2 R_{2S}(z, k)], \quad (4.1)$$

where α is the fine structure constant, k is the photon energy in units of the electron rest energy, P_K and P_{L_1} are the relative capture probabilities for electrons in 1S and 2S shell, respectively, $R_{ns}(z, k)$ are the relativistic correction factors and k_{max}^{ns} are the end-point energies of the partial nS -IB spectra. k_{max}^{ns} is equal to $Q_{EC} - k_B^{ns}$ where Q_{EC} is the transition energy and k_B^{ns} is the binding energy of the captured nS electron. The correction factors $R_{1S}(z, k)$ and $R_{2S}(z, k)$ were calculated from Martin-Glauber theory [Eqs. (4.5a) and (4.5b) in Ref. 8 and Eqs. (9.16) and (9.25) in Ref. 7, respectively] and from the improved calculations presented by Intemann.

In our calculations of the IB spectrum we used for Q_{EC} a value of 861.75 ± 0.09 keV obtained from the most recent atomic mass tables.²⁷ Experimental values of the relative capture probabilities P_K and P_{L_1} for 1S and 2S orbital electrons in ${}^7\text{Be}$ are not available. The theoretical results for the

ratio P_{L_1}/P_K are 0.033²⁸ and 0.039,²⁹ which change to values between 0.11 and 0.15 if exchange-overlap correction introduced by Bahcall³⁰ are applied. The L electrons in Be metal are found, to a large extent, in p -type orbital states.^{31,32} In this case, the capture rate for 2S electrons must be reduced compared with the theoretical values. A similar reduction in the population of 2S states is expected for Be compounds for the ^7Be half-life measured in various ^7Be compounds and metallic ^7Be are found to differ only slightly.^{33,34} So we adopted, following Mutterer,¹² a value of 0.07 ± 0.07 for P_{L_1}/P_K and accordingly 0.935 ± 0.065 for P_K and 0.065 ± 0.065 for P_{L_1} . These values take into account the chemical effects on the IB yield and give rise to an error of $\sim 0.8\%$ on $W_{\text{IB}}^{\text{th}}(k)$.

For comparing the measured 1S + 2S IB spectrum with theory Eq. (1) can be written in another form by introducing $W_{\text{IB}}^{\text{CF}}(k, k_{\text{max}}^{1S})$; the result of the earlier Coulomb-free approach of Morrison and Schiff as

$$W_{\text{IB}}^{\text{th}}(k) dk = R_S(z, k) W_{\text{IB}}^{\text{CF}}(k, k_{\text{max}}^{1S}) dk, \quad (4.2)$$

$$W_{\text{IB}}^{\text{CF}}(k, k_{\text{max}}^{1S}) dk = \frac{\alpha}{\pi} k (1 - k/k_{\text{max}}^{1S})^2 dk. \quad (4.3)$$

The function $R_S(z, k)$ which can be defined as the overall shape factor for the S-IB spectrum is given by

$$R_S(z, k) = P_K R_{1S}(z, k) + P_{L_1} R_{2S}(z, k) h(k). \quad (4.4)$$

The function $h(k)$ introduced in Eq. (4.4) corrects for the difference in binding energy of the 1S and 2S electrons ($k_B^{1S} - k_B^{2S} \approx k_{KX}$) and is given by

$$h(k) \approx [1 + k_{KX}/(k_{\text{max}}^{1S} - k)]^2. \quad (4.5)$$

Figure 4 shows the comparison of the measured IB pulse-height spectrum $W_{\text{IB}}^{\text{exp}}(k)$ per ground state EC decay of ^7Be obtained as the average of five corrected consistent IB spectra, with the theoretical spectrum [Eq. (4.2)] normalized to an energy interval of 1 keV. Numerical results of integral rates $N_{\text{IB}}(E_1) = \int_{E_1}^{Q_{\text{EC}}} W_{\text{IB}}(k) dk$ are listed in Table I for various low energy limits E_1 . The integral IB intensity obtained by integrating $W_{\text{IB}}^{\text{exp}}(k)$ over the energy range $560 \text{ keV} \leq k \leq Q_{\text{EC}}$ is compared in Table II with corresponding theoretical values.

Figure 5 shows the overall shape factor $R_S(z, k)$ for S-IB [Eq. (4.2)] as a function of photon energy. It is easy to see from this figure that the accuracy of the data is not sufficient to establish conclusively the energy dependence of $R_S(z, k)$. More precise measurements covering a wider energy range are required for that purpose.

V. ERROR ANALYSIS

The corrections to the measured IB pulse-height distribution are due only to finite energy resolu-

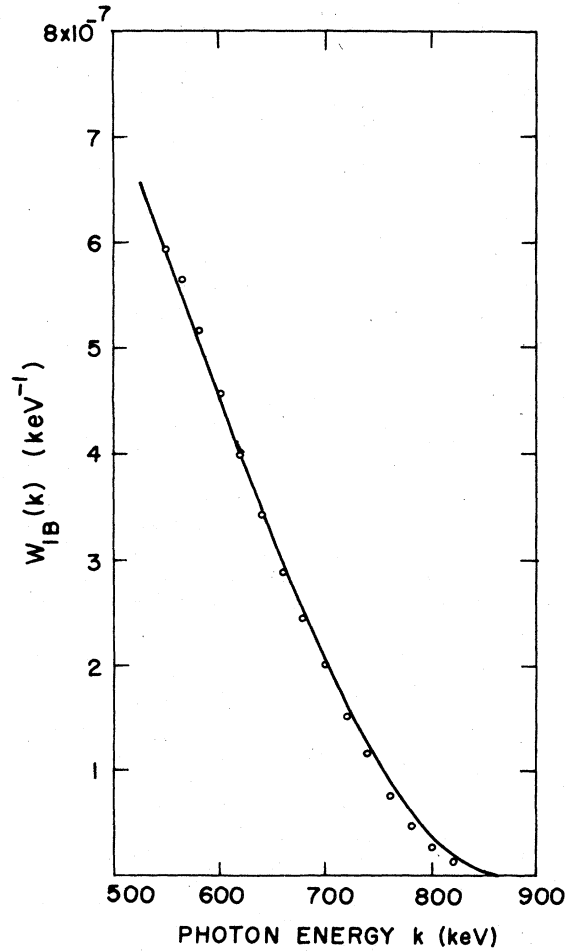


FIG. 4. Pulse-height spectrum $W_{\text{IB}}(k)$ of ^7Be IB photons per ground state EC decay. The open circles (ooo) show the experimental spectrum; the full line represents the theoretical spectrum calculated from Glauber-Martin theory.

tion, Compton electron distribution, detection efficiency, and pileup effect. The corrections due to finite energy resolution and Compton electron distribution in the energy region of present measurement are negligible and so the contributions

TABLE I. Measured IB counting rates $N_{\text{IB}}^{\text{exp}}(E_1)$ per ground state EC decay of ^7Be , compared with those calculated from the theoretical spectrum (see Fig. 4).

E_1 (keV)	$N_{\text{IB}}^{\text{exp}}(E_1)$ (per 10^6 ground state EC decay of ^7Be)	$N_{\text{IB}}^{\text{th}}(E_1)$
560-840	63.1 ± 3.8	64.6 ± 0.7
600-840	42.5 ± 2.9	44.2 ± 0.5
660-840	20.2 ± 1.7	21.8 ± 0.2
700-840	10.5 ± 1.1	11.7 ± 0.1
760-840	2.4 ± 0.3	3.3 ± 0.05

TABLE II. Ratios of measured to predicted IB yields in ⁷Be.

Decay	Transition energy (keV)	Energy range (keV)	Exp.-to-theor. IB yield ^a with theor. values of Martin, Glauber, and Intemann	References
⁷ Be(EC) ⁷ Li*	384.1 ± 0.1			27
	388 ± 8	50-360	1.12 ± 0.08	
		100-360	1.18 ± 0.09	14
		120-360	1.21 ± 0.10	
⁷ Be(EC) ⁷ Li	395 ± 25	120-360	0.77 ± 0.17	13
	861.75 ± 0.09			27
	851 ± 12	523.7-861.7	1.05 ± 0.08	12
	857 ± 14	560 -840	0.98 ± 0.05	Present work

^aThe theoretical values were calculated with $Q_{EC} = 861.75 \pm 0.09$ keV. The quoted errors correspond to the sum of the experimental errors on the theoretical values (see text).

to the error from these corrections are not considered. More than 80% of the contribution to the pileup spectrum comes from the photopeak region of the 478 keV nuclear γ rays. Since the counting rate in this region is comparatively very large, the statistical error becomes very small. As a result the overall error on the pileup spectrum becomes trivial ($\leq 0.1\%$). Only correction due to detection efficiency contributes to the final error on the IB spectrum. This is found to be 3-5% in the energy region 500-850 keV.¹⁹ The other source of error is due to counting statistics. This is restricted to 3-5% in the entire region of the measured IB by properly increasing the counting time with increasing energy. Therefore the total or rms error in the experimental IB intensity is

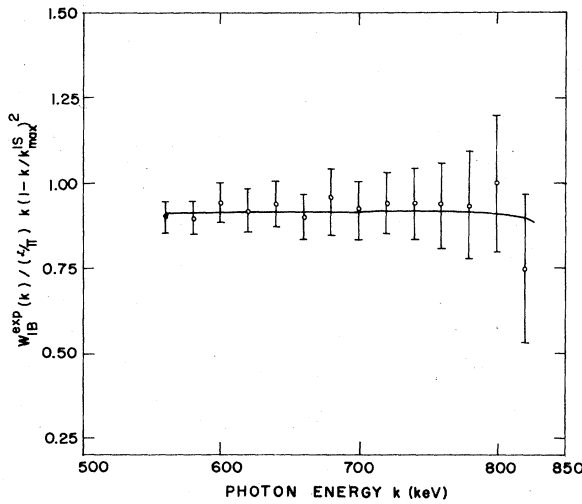


FIG. 5. The overall shape factor of the ⁷Be IB spectrum in the energy region 560-820 keV. The open circles (ooo) show the experimental points; the full line represents the theoretical prediction according to Eq. (4.24).

around 6%, as one can see from Table I.

The error on the end-point energy was obtained by the least-squares fit analysis of the data. The errors on the theoretical rates, given in Table I, are composed of the errors due to P_L/P_R (0.8%) and Q_{EC} (0.1%).

VI. TRANSITION ENERGY

Equation (4.2) is used to determine the end-point energy of 1S-IB spectrum by constructing the

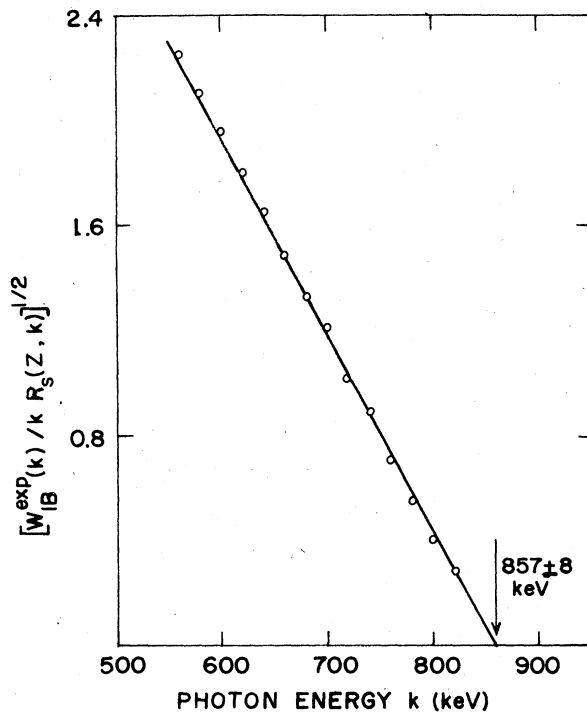


FIG. 6. Jauch plot, $W_{IB}^{exp}(k)/kR_S(z, k)^{1/2}$ vs k , of the IB spectrum of ⁷Be, yielding an end-point energy of 857 ± 8 keV.

Jauch plot³⁵ to the measured IB spectrum according to

$$[W_{\text{IB}}^{\text{xp}}(k)/kR_S(z, k)]^{1/2} = (\alpha/\pi)^{1/2} \left(1 - \frac{k}{k_{\text{max}}^{1S}} \right). \quad (6.1)$$

Figure 6 is the resulting Jauch plot which yields an IB end-point energy of 857 ± 8 keV. If the energy dependence of the relativistic correction factors is neglected by setting $R_{1S} = R_{2S} = 1$, the data yields an end-point energy of 851 ± 8 keV. Since the energy dependence of the correction factors is not yet experimentally established the difference of 6 keV is considered as an additional systematic error. The transition energy of ${}^7\text{Be}$ is therefore $Q_{\text{EC}} = 857 \pm 14$ keV. This value is in good agreement with the accepted mass difference.²⁷

VII. RESULTS AND DISCUSSION

The present measurements confirm the prediction of the theory of Martin and Glauber for allowed radiative capture of 1S+2S orbital electrons in the higher energy region of the IB spectrum. The measured 1S-IB end-point energy is in close agreement with the accepted atomic mass difference.²⁷ The confirmation of the predicted ratio of the radiative to ordinary nonradiative EC by the present measurements is consistent with the measurements of Mutterer¹² and that of 1S-IB K x ray coincidence in a heavier nuclide ${}^{165}\text{Er}$.³⁶

However, it is in contradiction to recent experiments on ${}^{51}\text{Cr}$,³⁷ ${}^7\text{Be}$,^{13,14} ${}^{54}\text{Mn}$,¹⁴ and ${}^{57}\text{Co}$.³⁸ With one exception,¹⁵ these were IB- γ coincidence experiments with NaI detectors in face-to-face geometry. IB- γ coincidence measurement is complicated by scattering between the crystals. This is likely to lead to an overestimation of chance coincidences. Coincidences between IB and nuclear γ rays which differ in intensities by about 10^{-4} are also likely to further complicate the measurements.

The approximations made by Martin and Glauber to calculate the IB spectrum accompanying allowed electron capture decays are fairly reliable for lighter elements. This is borne out by the exact calculations of Intemann in the case of EC decay of ${}^7\text{Be}$. The difference between these two calculations is only 0.5%. Intemann's calculations yield an increase of the 1S-IB intensity and a decrease of the 2S-IB intensity which aggregate to zero in the total 1S+2S spectrum.

VIII. ACKNOWLEDGMENT

We thank Professor V. Lakshminarayana of Andhra University, Waltair, for making available the Ge(Li) spectra of the ${}^7\text{Be}$ sources used in our measurements. We express our indebtedness to Dr. M. Mutterer for making available to us the preprint of a review article (Ref. 6) on radiative electron capture.

-
- ¹C. Moller, Phys. Z. Sowjetunion **11**, 9 (1937); Phys. Rev. **51**, 84 (1937).
²P. Morrison and L. I. Schiff, Phys. Rev. **58**, 24 (1940).
³H. Bradt, P. C. Gugelot, O. Huber, H. Medicus, P. Preiswerk, P. Scherrer, and R. Steffen, Helv. Phys. Acta **19**, 222 (1946).
⁴C. S. Wu, in *Beta- and Gamma-Ray Spectroscopy*, edited by K. Siegbahn (North-Holland, Amsterdam, 1955), p. 649.
⁵B. G. Peterson, in *Alpha-, Beta-, and Gamma-Ray Spectroscopy*, edited by K. Siegbahn (North-Holland, Amsterdam, 1965), Vol. 2, p. 1574.
⁶W. Bombynek, H. Behrens, M. H. Chen, B. Crasemann, M. L. Fitzpatrick, K. W. D. Ledingham, H. Genz, M. Mutterer, and R. L. Intemann, Rev. Mod. Phys. **49**, 77 (1977).
⁷R. J. Glauber and P. C. Martin, Phys. Rev. **104**, 158 (1956).
⁸P. C. Martin and R. J. Glauber, Phys. Rev. **109**, 1307 (1958).
⁹R. L. Intemann, Phys. Rev. C **3**, 1 (1971).
¹⁰B. A. Zon and L. P. Rapaport, Yad. Fiz. **7**, 528 (1968) [Sov. J. Nucl. Phys. **7**, 330 (1968)].
¹¹I. Kadar, D. Berenyi, and B. Myslek, Nucl. Phys. **A153**, 383 (1970).
¹²M. Mutterer, Phys. Rev. C **8**, 2089 (1973).
¹³H. Laneman and J. M. Lebowitz, Phys. Rev. C **3**, 465 (1971).
¹⁴B. I. Persson and S. E. Koonin, Phys. Rev. C **5**, 1443 (1972).
¹⁵J. C. Vanderleeden, F. Boehm, and E. D. Lipson, Phys. Rev. C **4**, 2218 (1971).
¹⁶A. Spornol, E. De Roost, and M. Mutterer, Nucl. Instrum. Methods **112**, 169 (1973).
¹⁷P. Quittner, *Gamma-Ray Spectroscopy* (Adam Hilger Ltd, London, 1972), p. 96.
¹⁸R. L. Heath, Scintillation Spectrometry, Gamma-Ray Spectrum Catalogue IDO-16880-1 (unpublished), 2nd ed.
¹⁹K. Narasimhamurthy and S. Jnanananda, Proc. Phys. Soc. **90**, 109 (1967).
²⁰K. Liden and N. Starfelt, Ark. Fys. **7**, 427 (1954); Phys. Rev. **97**, 419 (1955).
²¹D. Berenyi and D. Varga, Acta Phys. Acad. Sci. Hung. **29**, 1 (1970).
²²W. R. Dixon and J. H. Attken, Can. J. Phys. **36**, 1624 (1958).
²³G. E. Owen and H. Primakoff, Phys. Rev. **74**, 1406 (1948).
²⁴J. P. Palmer and L. J. Laslett, AEC Report No. 1220, 1951 (unpublished).
²⁵H. Lentz and G. Schulz, Nucl. Instrum. Methods **40**, 257 (1966).
²⁶E. A. Wolicki, R. Jastrow, and F. D. Brooks, NRL Report No. NRL-4833, 1956 (unpublished).

- ²⁷A. H. Wapstra and N. B. Gove, Nucl. Data A9, 267 (1971).
- ²⁸G. Winter, Nucl. Phys. A113, 617 (1968).
- ²⁹L. N. Zyryanova and Yu. P. Suslov, Izv. Akad. Nauk SSSR Ser.-Fiz. 33, 1693 (1969) [Bull. Acad. Sci. USSR Phys. Ser.- 33, 1553 (1969)].
- ³⁰J. N. Bahcall, Nucl. Phys. 71, 267 (1968); E. Vatai, *ibid.* A156, 541 (1970); P. H. Blichert-Toft, Nucl. Data A8, 160 (1970).
- ³¹M. Pomerantz and T. P. Das, Phys. Rev. 119, 70 (1960).
- ³²W. C. Phillips and R. J. Weiss, Phys. Rev. 171, 790 (1968).
- ³³H. W. Johlige, D. C. Aumann, and H. J. Born, Phys. Rev. C 2, 1616 (1970).
- ³⁴E. Vatai and Cs. Ujhelzi, USAEC Report No. CONF-720404, 1973 (unpublished), Vol. 3, p. 2030.
- ³⁵J. M. Jauch, ORNL Report No. ORNL-1102, 1951 (unpublished).
- ³⁶Z. Sujkowski, J. Jastrzebski, A. Zglinski, and J. Zylicz, in *Proceedings of the International Conference on the Role of Atomic Electrons in Nuclear Transformations, Warsaw, Poland, 24-28 Sept., 1963* (Nuclear Energy Information Center, Warsaw, Poland, 1965), Vol. IV, p. 614.
- ³⁷S. E. Koonin and B. I. Persson, Phys. Rev. C 6, 1713 (1972).
- ³⁸H. Laneman and J. M. Lebowitz, Phys. Rev. C 3, 188 (1971).